Preprint typeset in JHEP style. - HYPER VERSION

hep-th/0108182
AEI-2001-106

Two Loops to Two Loops in $\mathcal{N} = 4$ Supersymmetric Yang-Mills Theory

Jan Plefka and Matthias Staudacher

Albert-Einstein-Institut, Max-Planck-Institut für Gravitationsphysik
Am Mühlenberg 1, D-14476 Golm, Germany
Email: plefka,matthias@aei-potsdam.mpg.de

Abstract: We present a full two-loop $\mathcal{O}(g^6)$ perturbative field theoretic calculation of the expectation value of two circular Maldacena-Wilson loops in $D = 4$ $\mathcal{N} = 4$ supersymmetric $U(N)$ gauge theory. It is demonstrated that, after taking into account very subtle cancellations of bulk and boundary divergences, the result is completely finite without any renormalization. As opposed to previous lower order calculations existing in the literature, internal vertex diagrams no longer cancel identically and lead to subleading corrections to the dominant ladder diagrams. Taking limits, we proceed to extract the two-loop static potential corresponding to two infinite anti-parallel lines. Our result gives some evidence that the existing strong-coupling calculations using the AdS/CFT conjecture might sum up the full set of large N planar Feynman diagrams.

Keywords: AdS-CFT Correspondence; Duality in Gauge Field Theories; Extended Supersymmetry; NLO Computations.

Contents

1. Introduction and Conclusions

Interest in 't Hooft's 1973 proposal [1] to consider the limit $N \to \infty$ of $U(N)$ quantum gauge theory such that $\lambda = Ng^2$ stays finite is not waning even after nearly thirty years of, to date, futile attempts to analytically perform the sum over the resulting planar Feynman diagrams. In the original work it was already conjectured that an indirect approach using string theory might be more likely to succeed. The first-ever concrete suggestion for formulating such a string theory "dual" to the very special four-dimensional gauge theory invariant under $\mathcal{N} = 4$ supersymmetries has been made by Maldacena [2]. In its most modest form the conjecture holds that the limit of strong 't Hooft coupling $\lambda \to \infty$ in the $N = \infty$ gauge theory is reproduced by the low energy supergravity limit of IIB string theory in the background $\mathrm{AdS}_5 \times S^5$. This proposal does lead to very explicit, analytic predictions for the large N and λ limit of various observables in the gauge theory. It is usually believed that instanton effects are inessential at $N = \infty$; therefore the predictions should coincide with the two-step procedure of first calculating the observables in question to all orders in planar perturbation theory and, barring large N phase transitions, subsequently taking the large λ limit of the resulting sum. Our inability, however, of actually carrying through this program constituted the chief motivation for seeking a dual

formulation in the first place. In short, we are in the frustrating situation of being presented with a proposed solution of a notorious problem without being able to prove that the solution is indeed correct!

Recently, there has been some interesting progress towards making much more direct contact between the Euclidean $\mathcal{N} = 4$ gauge theory and its suggested supergravity dual. In [3] Maldacena introduced a non-local loop operator, which differs from the usual Wilson loop in a subtle way: In addition to the gauge field the six scalars of the model are also coupled to the loop C. The coupling is such that the new operator $\mathcal{W}[C]$, which we will call a Maldacena-Wilson loop operator, is no longer unitary and its magnitude is thus no longer bounded by one (see eq.(2.1) for a precise definition). A priori it is therefore not even clear whether the expectation value of this operator exists. AdS/CFT, for various types of contours C, leads to some very explicit results [3],[4], see also [5]. A straight infinite line e.g. is a BPS object and should satisfy

$$\langle \mathcal{W}[C] \rangle = 1, \qquad C = \text{straight line}. \tag{1.1}$$

Furthermore, in the double limit $N \to \infty$, $\lambda = Ng^2 \to \infty$ one finds for a circular contour, independently of the radius,

$$\langle \mathcal{W}[C] \rangle = e^{\sqrt{\lambda}}, \qquad C = \text{circle}. \tag{1.2}$$

Finally for a rectangular Maldacena-Wilson loop of sides $T \times L$ the prediction reads, for $N = \infty$, $\lambda \to \infty$ and $T \to \infty$,

$$\langle \mathcal{W}[C] \rangle = \exp\left(\frac{4\pi^2}{\Gamma^4(1/4)}\sqrt{\lambda}\frac{T}{L}\right). \qquad C = \text{rectangle}, \tag{1.3}$$

which may be used to define the so-called static potential $V(L) = -1/T \log\langle \mathcal{W}[C] \rangle$.

In [6],[7] the authors pioneered the weak coupling, perturbative analysis of Maldacena-Wilson loops. They found that up to one-loop order (i.e. $\mathcal{O}(g^4)$) all Feynman diagrams cancel for a straight line, as is required if eq.(1.1) is to hold in the gauge theory. Furthermore, for a circle and a rectangle (with $T \to \infty$, i.e. infinite anti-parallel lines) all non-ladder diagrams (i.e. containing internal interaction vertices) cancel. The authors went on to sum up ladder diagrams to all orders for the circle and the anti-parallel lines. Interestingly, for $N = \infty$ (planar ladders) and for the circle they found *exactly* eq.(1.2), while the anti-parallel lines yielded something very similar to eq.(1.3):

$$\langle \mathcal{W}[C] \rangle_{\text{ladder approx.}} = \exp\left(\frac{1}{\pi}\sqrt{\lambda}\frac{T}{L}\right). \qquad C = \text{rectangle}. \tag{1.4}$$

Closer inspection of these calculations reveals a number of interesting features:

• The celebrated $\sqrt{\lambda}$ strong coupling "screening" behavior of eqs.(1.2),(1.3) is seen to be a large N artifact: If one looks at the ladder approximation at *finite* N one easily proves that the behavior is always $\sim \exp g^2 \sim \exp \lambda/N$. Incidentally, the ladder approximation has been argued to be exact for a circle even at finite N and λ [8]. If true, the result for, say, $SU(2)$ would read

$$\langle \mathcal{W}[C] \rangle_{\mathrm{SU(2)}} = (1 + \frac{1}{8} g^2)\ e^{\frac{1}{16} g^2} \qquad C = \text{circle}. \tag{1.5}$$

• Individual non-ladder diagrams are divergent. After adding all interactive diagrams the divergences cancel. It is particularly intriguing that some divergent contact interactions at the boundaries of the loops (which are present in an ordinary unitary Wilson loop, even in $\mathcal{N} = 4$ theory) are precisely canceled by a bulk divergence in the supersymmetric self-energy. This demonstrates that the Maldacena-Wilson loop might turn out to be a field theoretic observable that is finite to all orders in perturbation theory! A proof of this is, however, currently lacking.
• For the circle the ladder approximation reproduces the AdS/CFT strong coupling result, which is consistent with it being exact. For the anti-parallel lines we notice by comparing eq.(1.3) and eq.(1.4) that the result is qualitatively, but not quantitatively correct. Turning this around we see that AdS/CFT *predicts* that non-ladder diagrams must contribute to the static potential: The cancellation mechanism of internal vertex diagrams at $\mathcal{O}(g^4)$ found in [6],[7] should not extend to all orders in perturbation theory, for in that case the AdS/CFT correspondence, in its current form, would be proven wrong.

In the present paper we are aiming at extending and deepening the results of [6],[7]. Clearly one should perform a two-loop calculation in order to investigate whether internal vertex diagrams begin to contribute, as well as to further test the finiteness of the Maldacena-Wilson loop. Unfortunately the number of diagrams relevant to the so far mentioned contours is discouragingly large. We therefore found it convenient to study a slightly different situation which nevertheless allows to gain new insight: We will consider two closed, axisymmetric, parallel circles. As will be shown in the following section a large number of diagrams are zero for group theoretic reasons and a two-loop calculation becomes feasible (see the figure in section 2 for the relevant diagrams). The configuration of two circular loops has been studied before in the literature. Strong-coupling supergravity computations were done in [9], and it was found, notably, that the limit of very large, nearby circles exactly reproduces the anti-parallel lines potential of eq.(1.3). Furthermore, the sum over all ladder diagrams for this situation was obtained in [10], reproducing, in the anti-parallel lines limit, the result of eq.(1.4). Hence from the strong-coupling perspective our scenario of two parallel, axisymmetric circles does not seem to differ from the anti-parallel lines situation in the static potential limit.

Despite the considerable reduction of the number of diagrams mentioned above our two-loop perturbative calculation is quite lengthy and will be presented below.

We decided to detail some of the techniques employed since they might be found useful for further investigations.

For our geometry we are able to exhibit the complete finiteness of the Maldacena-Wilson loop up to $\mathcal{O}(g^6)$. Some interactive diagrams (see the X- and H-graphs in sections 3.4 and 3.5) are superficially divergent due to contact interactions at the circular boundaries. However, due to the special nature of the loop operator the divergent contributions cancel between gauge and scalar degrees of freedom. An even more intricate cancellation takes place between a divergent "bulk" self-energy contribution (section 3.2) and a divergent "boundary" contact interaction (the IY-graph in section 3.3), repeating a phenomenon first discovered in [7]. We find this perturbative finiteness of the Maldacena-Wilson observable quite remarkable; it certainly deserves a deeper understanding.

Adding the finite contributions of all non-ladder diagrams we establish that, to two-loop order, *they no longer cancel*. For finite geometry, this requires some numerical analysis in the final steps. Taking, in section 4, the limit of very large, near-by circles we analytically complete the computation and extract the static potential limit corresponding to infinite anti-parallel lines[1]. It is then proved that the vertex-diagrams contribute in a weak, but non-vanishing fashion. We will end by discussing whether these weak, non-zero corrections to the ladder approximation might be of help in explaining the discrepancy between eqs.(1.3) and (1.4).

In an outlook (section 5) we collect some of the exciting unsolved mysteries surrounding Maldacena-Wilson loops.

2. The Graphs and the Computation to Order g^2 and g^4

An interesting modification of the standard (Euclidean) Wilson loop operator, appropriate for $\mathcal{N} = 4$ gauge theory, was introduced in [3]. Its transformation properties under supersymmetry were elucidated in [11]. It couples not only to the gauge potentials $A_\mu(x)$, but also to the six scalar fields $\Phi_I(x)$ of $\mathcal{N} = 4$ SYM theory

$$\mathcal{W}[C] = \mathrm{Tr}\ \mathrm{P} \exp\Big[\oint_C d\tau (iA_\mu(x)\dot{x}^\mu + \Phi_I(x)\theta^I|\dot{x}|)\Big] \tag{2.1}$$

Here θ^I is a point on the unit five-sphere, i.e. $\theta^I\theta^I = 1$, and $x^\mu(\tau)$ parameterizes the curve C. The gauge field and the scalars are in the fundamental representation of $U(N)$ with generators T^a $(a = 0, \ldots, N^2 - 1)$, which we normalize according to $\mathrm{Tr}\ T^a T^b = \frac{1}{2}\delta^{ab}$ and which obey the $U(N)$ algebra

$$[T^a, T^b] = if^{abc}T^c \tag{2.2}$$

[1]Due to the circular boundary conditions our static potential result differs to $\mathcal{O}(g^4)$ from the perturbative calculations of [6],[7]. As mentioned above, this difference is a weak coupling feature that is expected to go away at strong coupling.

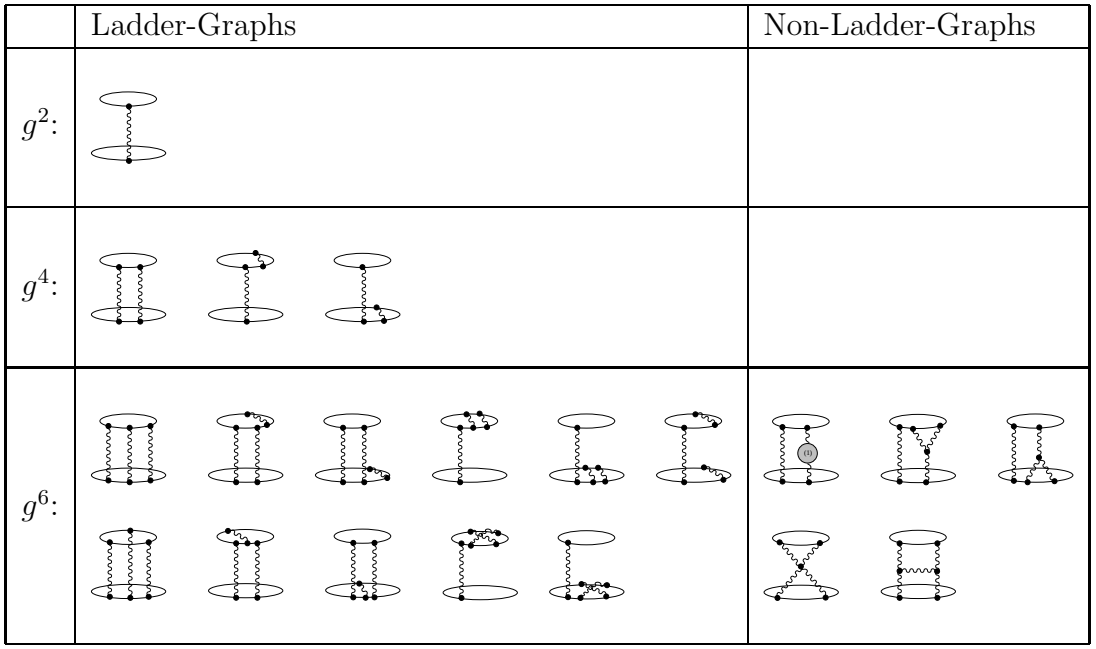

Figure 1: The connected nonvanishing graphs up to order g^6. The propagators stand for the combination of scalar and gluon exchange and the bubble denotes the one loop self-energy contribution. We will denote the non-ladder diagrams in the above figure by the self-energy, IY, IY^T, X and H-graph by obvious correspondence. Note that the g^6 ladder-graphs in the last line of the figure are non-planar.

Note that Tr $T^a = \sqrt{\frac{N}{2}}\delta^{a0}$, $f^{0bc} = 0$ as well as $f^{abc}f^{abc} = N(N^2-1)$. Due to the absence of an i in front of the scalar fields Φ_I in eq.(2.1) the Maldacena-Wilson operator differs from an ordinary Wilson operator in an important way: It is no longer a pure phase factor, and therefore not bounded in field space.

We employ the Euclidean action of $\mathcal{N}=4$ supersymmetric Yang-Mills theory

$$S = \tfrac{1}{2g^2}\int d^4x\Big[\tfrac{1}{2}\,(F^a_{\mu\nu})^2 + (D_\mu\Phi^a_I)^2 + i\bar\psi^a\gamma^\mu D_\mu\psi^a + if^{abc}\bar\psi^a\Gamma^I\Phi^b_I\psi^c \\ +\tfrac{1}{2}\,(f^{abc}\Phi^b_I\Phi^c_J)^2 + \partial_\mu\bar c^a\, D_\mu c^a + (\partial_\mu A^a_\mu)^2\Big] \tag{2.3}$$

in the Feynman gauge with ghosts c^a and $\bar c^a$. Here $D_\mu(\cdot)^a = \partial_\mu(\cdot)^a + f^{abc}A^b_\mu(\cdot)^c$, ψ^a is a sixteen component Majorana spinor and (γ^μ, Γ^I) are ten 16×16 Dirac matrices stemming from the reduction of the ten dimensional model.

We shall be interested in the connected correlator of *two* Maldacena-Wilson loops

$$\langle \mathcal{W}(C_1)\,\mathcal{W}(C_2)\rangle_c = \langle \mathcal{W}(C_1)\,\mathcal{W}(C_2)\rangle - \langle \mathcal{W}(C_1)\rangle\,\langle \mathcal{W}(C_2)\rangle \tag{2.4}$$

where we take the curves C_1 and C_2 to be two parallel, axisymmetric circles of opposite orientation and, respectively, radii R_1 and R_2 separated by a distance h

$$x^\mu(\tau) = (R_1\,\cos\tau,\quad R_1\,\sin\tau,\,0\,,\,0) \\ y^\mu(\sigma) = (R_2\,\cos\sigma, -R_2\,\sin\sigma,\,h\,,\,0) \qquad \tau,\sigma\in[0,2\pi] \tag{2.5}$$

Performing the diagrammatic expansion in this geometry up to order six in the coupling constant g it is seen that a large number of diagrams vanish identically by taking into account the following two identities

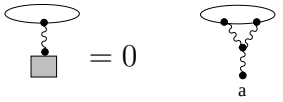

$$= 0 \qquad \sim f_{abc}\,\mathrm{Tr}\;T^b T^c = 0 \tag{2.6}$$

where the box in the first graph stands for any interaction vertex of the theory and the open leg of the second graph may be contracted with either interaction vertices or the second Wilson loop. Moreover at order g^6 the cancellation of

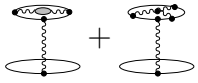

$$+ \qquad = 0 \tag{2.7}$$

may be taken into account, a consequence of the cancellation of the graphs with internal vertices for the circular loop at order g^4 shown in [7]. The remaining, highly reduced set of 20 non-vanishing planar and non-planar graphs is depicted in the figure.

Let us explicitly compute the leading one ladder graph at order g^2. The Feynman gauge propagators of the bosonic fields following from (2.3) are

$$\langle A^a_\mu(x)\,A^b_\nu(y)\rangle = g^2\frac{\delta^{ab}\,\delta_{\mu\nu}}{4\pi^2\,(x-y)^2} \qquad \langle \phi^a_I(x)\,\phi^b_J(y)\rangle = g^2\frac{\delta^{ab}\,\delta_{IJ}}{4\pi^2\,(x-y)^2}\,. \tag{2.8}$$

One then has

$$\begin{aligned} &= -g^2\,\mathrm{Tr}\;(T^a)\,\mathrm{Tr}\;(T^a)\int_0^{2\pi}\frac{d\tau\,d\sigma}{4\pi^2}\,\frac{\dot x\cdot\dot y-|\dot x|\,|\dot y|}{(x-y)^2} \\ &= \frac{g^2\,N}{4}\int_0^{2\pi}\frac{d\phi}{2\pi}\,\frac{1+\cos\phi}{\frac{R_1^2+R_2^2+h^2}{2\,R_1\,R_2}-\cos\phi} = -\frac{g^2N}{4}\Big[1-\sqrt{\tfrac{(R_1+R_2)^2+h^2}{(R_1-R_2)^2+h^2}}\Big] \end{aligned} \tag{2.9}$$

where we have made use of the parameterization of (2.5).

Turning to the three graphs at g^4 one notices that there are no path ordering effects at this order, which means that the computation factorizes into products of one ladder graphs. Taking care of combinatoric factors one finds

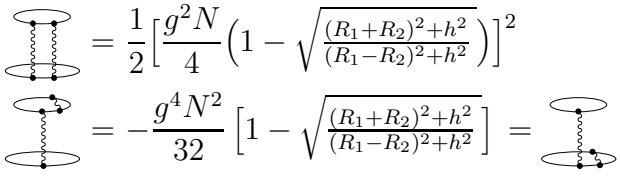

$$\begin{aligned} &= \frac{1}{2}\Big[\frac{g^2N}{4}\Big(1-\sqrt{\tfrac{(R_1+R_2)^2+h^2}{(R_1-R_2)^2+h^2}}\Big)\Big]^2 \\ &= -\frac{g^4N^2}{32}\Big[1-\sqrt{\tfrac{(R_1+R_2)^2+h^2}{(R_1-R_2)^2+h^2}}\Big] = \end{aligned} \tag{2.10}$$

for the diagrams at order g^4.

3. Order g^6

3.1 The Ladder Graphs

At order g^6 the computation becomes more challenging. Whereas the two and one ladder diagrams remain easy

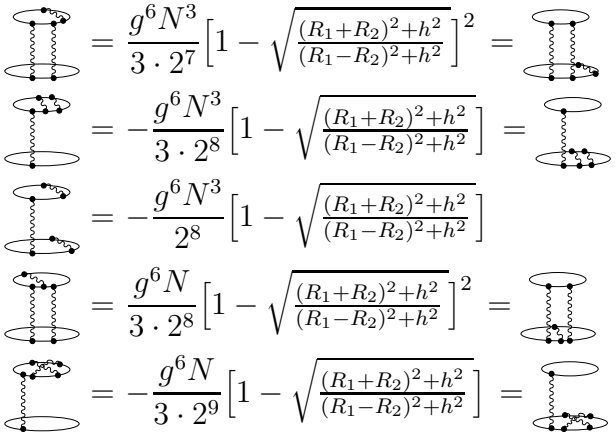

$$
\begin{aligned}
&= \frac{g^6N^3}{3\cdot 2^7}\Big[1-\sqrt{\tfrac{(R_1+R_2)^2+h^2}{(R_1-R_2)^2+h^2}}\,\Big]^2 = \\
&= -\frac{g^6N^3}{3\cdot 2^8}\Big[1-\sqrt{\tfrac{(R_1+R_2)^2+h^2}{(R_1-R_2)^2+h^2}}\,\Big] = \\
&= -\frac{g^6N^3}{2^8}\Big[1-\sqrt{\tfrac{(R_1+R_2)^2+h^2}{(R_1-R_2)^2+h^2}}\,\Big] \\
&= \frac{g^6N}{3\cdot 2^8}\Big[1-\sqrt{\tfrac{(R_1+R_2)^2+h^2}{(R_1-R_2)^2+h^2}}\,\Big]^2 = \\
&= -\frac{g^6N}{3\cdot 2^9}\Big[1-\sqrt{\tfrac{(R_1+R_2)^2+h^2}{(R_1-R_2)^2+h^2}}\,\Big] =
\end{aligned}
\tag{3.1}
$$

the three ladder graph requires considerably more care. One has

$$
\begin{aligned}
&= \tfrac{g^6N^3}{3\cdot 2^6}\int_0^{2\pi}\frac{d\phi}{2\pi}\frac{d\theta_1}{2\pi}\frac{d\theta_2}{2\pi}\int_0^{\theta_1}\frac{d\psi_1}{2\pi}\int_0^{\theta_2}\frac{d\psi_2}{2\pi}\times \\
&\qquad\times\frac{1+\cos\phi}{\kappa-\cos\phi}\;\frac{1+\cos(\psi_1+\theta_2+\phi)}{\kappa-\cos(\psi_1+\theta_2+\phi)}\;\frac{1+\cos(\psi_2+\theta_1+\phi)}{\kappa-\cos(\psi_2+\theta_1+\phi)}
\end{aligned}
\tag{3.2}
$$

where we have abbreviated $\kappa := \frac{R_1^2+R_2^2+h^2}{2\,R_1R_2}$. It is convenient to change to complex coordinates $(z, z_1, z_2, w_1, w_2) = (e^{i\phi}, e^{i\theta_1}, e^{i\theta_2}, e^{i\psi_1}, e^{i\psi_2})$ and to introduce the auxiliary parameter a through $\kappa := \frac{1}{2}(a+a^{-1})$. Then the integrations on w_1, w_2 are elementary and we obtain a triple contour integral:

$$
\begin{aligned}
&= \tfrac{g^6N^3}{3\cdot 2^6(2\pi)^2}\oint\frac{dz}{2\pi iz}\frac{dz_1}{2\pi z_1}\frac{dz_2}{2\pi z_2}\frac{(z+1)^2}{(z-a)(z-a^{-1})}\times \\
&\qquad\times\Big[\log z_1-\frac{1+a}{1-a}\log\frac{zz_1z_2-a}{zz_2-a}-\frac{1+a}{1-a}\log\frac{1-azz_2}{1-azz_1z_2}\Big]\times \\
&\qquad\times\Big[\log z_2-\frac{1+a}{1-a}\log\frac{zz_1z_2-a}{zz_1-a}-\frac{1+a}{1-a}\log\frac{1-azz_1}{1-azz_1z_2}\Big]
\end{aligned}
\tag{3.3}
$$

Carefully keeping track of the cuts introduced by the logarithms the integrals may be computed term-by-term with the help of Dilogarithms:

$$
\begin{aligned}
&= \tfrac{g^6N^3}{12}\Bigg\{\Big[-\frac{1}{4}\Big(1-\sqrt{\tfrac{(R_1+R_2)^2+h^2}{(R_1-R_2)^2+h^2}}\,\Big)\Big]^3 \\
&\qquad -\frac{3}{2^5\pi^2}\Big[1-\sqrt{\tfrac{(R_1+R_2)^2+h^2}{(R_1-R_2)^2+h^2}}\,\Big]\,\tfrac{(R_1+R_2)^2+h^2}{(R_1-R_2)^2+h^2}\;\mathrm{Li}_2(a^2)\Bigg\}
\end{aligned}
\tag{3.4}
$$

$$
\text{where}\qquad a^2=\frac{\Big(h^2+R_1^2+R_2^2-\sqrt{(h^2+R_1^2+R_2^2)^2-4R_1^2R_2^2}\Big)^2}{4R_1^2R_2^2}
$$

The non-planar cousin of the three ladder diagram is obtained by the same methods and reads

$$= \frac{g^6 N}{12} \Big\{ \Big[-\frac{1}{4} \Big(1 - \sqrt{\tfrac{(R_1+R_2)^2+h^2}{(R_1-R_2)^2+h^2}} \Big) \Big]^3 + \frac{3}{2^5 \pi^2} \Big[1 - \sqrt{\tfrac{(R_1+R_2)^2+h^2}{(R_1-R_2)^2+h^2}} \Big] \tfrac{(R_1+R_2)^2+h^2}{(R_1-R_2)^2+h^2} \; \mathrm{Li}_2(a^2) \Big\} . \tag{3.5}$$

3.2 The Self-Energy Graph

$\mathcal{N} = 4$ gauge theory is a finite theory. This, however, does not mean that gauge dependent, individual Feynman diagrams are finite as well. An important example are the self energies of the gauge bosons and scalars, which are infinite in four dimensions. In order to isolate the divergences we use regularization by dimensional reduction which maintains supersymmetry. This procedure considers supersymmetric Yang-Mills theory in 2ω dimensions as a dimensional reduction of the ten dimensional model. One hence has a 2ω component gauge field A^a_μ, $10 - 2\omega$ scalars and a 16 component fermion field at every stage of the computation. The one-loop self energy of the vector and scalar fields was computed in this regularization in [7]. In configuration space one has

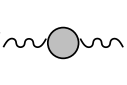

$$= \delta_{\mu\nu}\, \delta^{\tilde{a}\tilde{b}}\, g^4 N\, A_\omega[x] + \frac{\delta^{\tilde{a}\tilde{b}}\, g^4 N\, \Gamma^2(\omega-1)}{2^7 \pi^{2\omega}\, (\omega-2)^2\, (\omega-3)\, (2\omega-3)}\, \partial_{x^\mu} \partial_{x^\nu} \Big([x^2]^{4-2\omega} \Big)$$

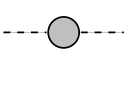

$$= \delta_{IJ}\, \delta^{\tilde{a}\tilde{b}}\, g^4 N\, A_\omega[x] \tag{3.6}$$

with group indices $\tilde{a}, \tilde{b} = 1, \ldots, N^2 - 1$ in the interacting $SU(N)$ sector and where the universal function $A_\omega[x]$ is given by

$$A_\omega[x] = \frac{\Gamma^2(\omega-1)}{2^5 \pi^{2\omega}\, (2-\omega)\, (2\omega-3)}\, \frac{1}{[x^2]^{2\omega-3}} \tag{3.7}$$

which diverges in four dimensions.

Turning toward the evaluation of the self-energy graph itself we find

$$= \frac{4\, g^6 N}{2!\, 2!} \Big[\mathrm{Tr}\; (T^{\tilde{a}}\, T^{\tilde{b}}) \Big]^2 \int_0^{2\pi} d\tau_1\, d\sigma_1\, (\dot{x}_1 \cdot \dot{y}_1 - |\dot{x}_1|\, |\dot{y}_1|) \Delta_\omega[x_1(\tau_1) - y_1(\sigma_1)] \times \int_0^{2\pi} d\tau_2\, d\sigma_2\, (\dot{x}_2 \cdot \dot{y}_2 - |\dot{x}_2|\, |\dot{y}_2|)\, A_\omega[x_2(\tau_2) - y_2(\sigma_2)] \tag{3.8}$$

Here Δ_ω denotes the propagator (2.8) in 2ω dimensions with stripped off coupling constant and Kronecker delta-functions

$$\Delta_\omega(x) = \frac{\Gamma(\omega-1)}{4\pi^\omega}\, \frac{1}{[x^2]^{\omega-1}}\, . \tag{3.9}$$

We stress that the double derivative term in the vector self-energy of (3.6) drops out as it constitutes a total derivative here. However, at higher orders this inhomogenous

contribution to the one loop self-energy might become relevant. The self-energy graph (3.8) is divergent in 4d – this divergence will cancel against the IY graphs. We leave it as it stands for the time being, noting that the prefactor in (3.8) takes the value $g^6 N(N^2-1)/4$.

3.3 The IY-Graphs: Cancellation of Divergences

When evaluating the two IY-diagrams we encounter a second type of infinity distinct in origin from the type of "bulk" divergences discussed in the last subsection. When two of the three legs of the three-vertex come close on the boundary, the confluence causes a logarithmic "boundary" divergence. To be consistent, we regulate it by the same procedure of dimensional reduction used above. We then find that it cancels against the self-energy divergence. One furthermore needs to carefully extract the finite contribution next to the infinite piece, which is subtle and technically quite involved. In fact, we will only do this explicitly for the special case $R_1 = R_2$ – the finite part for the case of more general geometries is not needed for reaching our physical conclusions. Using the parameterization of (2.5) we denote the three points on the upper loop by $x_i(\tau_i)$ $(i = 1, 2, 3)$ and the two points on the lower loop by $y_j(\sigma_j)$ $(j = 1, 2)$. Path ordering only occurs for the upper loop in the τ_i parameters. Performing the usual Wick contractions one is confronted with the integral

$$= \tfrac{g^6\, N\,(N^2-1)}{8} \int_0^{2\pi} d\tau_1 d\tau_2 d\tau_3 \int_0^{2\pi} d\sigma_1 d\sigma_2\, \epsilon(\tau_1,\tau_2,\tau_3)\,(\dot{x}_3\cdot\dot{y}_1 - R_1\,R_2)\,\Delta_\omega(x_3-y_1)$$
$$\times\Big\{(\dot{x}_1\cdot\dot{y}_2 - R_1\,R_2)\,[\dot{x}_2\cdot\partial_{y_2} - \dot{x}_2\cdot\partial_{x_1}] - (\dot{x}_1\cdot\dot{x}_2 - R_1^2)\,\dot{y}_2\cdot\partial_{x_2}\Big\}\,G(x_1,x_2,y_2) \tag{3.10}$$

where an ordering symbol has been introduced obeying $\epsilon(\tau_1,\tau_2,\tau_3) = 1$ for $\tau_1 > \tau_2 > \tau_3$ and antisymmetric under any permutation of τ_i. Moreover we have defined the dimensional regulated three-point function

$$G(x_1,x_2,y_2) = \int d^{2\omega} r\,\Delta_\omega(x_1-r)\,\Delta_\omega(x_2-r)\,\Delta_\omega(y_2-r) \tag{3.11}$$

with $\Delta_\omega(x)$ given by (3.9). As the "I"-leg term $(\dot{x}_3\cdot\dot{y}_1 - R_1\,R_2)\,\Delta_\omega(x_3-y_1)$ depends homogeneously on the angular combination $(\sigma_1+\tau_3)$ a shift in the lower σ_1 integration by $\sigma_1 \to \sigma_1 - \tau_3$ lets the "I" leg of the IY-graph decouple. Then the only dependence on τ_3 in the integrand of (3.10) sits in the ordering symbol $\epsilon(\tau_1,\tau_2,\tau_3)$ and this integral may be performed to yield

$$\int_0^{2\pi} d\tau_3\,\epsilon(\tau_1,\tau_2,\tau_3) = 2\pi\,\mathrm{sgn}(\tau_1-\tau_2) - 2(\tau_1-\tau_2) \equiv E(\tau_1.\tau_2)\,. \tag{3.12}$$

In order to proceed one now introduces Feynman parameters for (3.11) and performs the integral over r. Collecting the dependence on the "I"-leg and the prefactor of

(3.10) in the symbol (I),

$$(\mathrm{I}) \equiv \frac{g^6\, N\,(N^2-1)}{16\pi} \int_0^{2\pi} d\tau\, d\sigma\, (\dot{x}\cdot\dot{y} - R_1 R_2)\Delta_\omega[x(\tau)-y(\sigma)] \tag{3.13}$$

the expression (3.10) takes the rather complicated form

$$\begin{aligned} &= (\mathrm{I})\,\frac{\Gamma(2\omega-2)}{2^5\pi^{2\omega}} \int_0^{2\pi} d\tau_1 d\tau_2 d\sigma_2 \int_0^1 d\alpha d\beta d\gamma\, (\alpha\beta\gamma)^{\omega-2}\,\delta(\alpha+\beta+\gamma-1)\, E(\tau_1,\tau_2) \\ &\times\Big\{-R_1R_2\,(1+\cos(\sigma_2+\tau_1))\,\Big[R_1R_2\sin(\sigma_2+\tau_2)\,(2\alpha+\beta)\gamma + {R_1}^2\sin\tau_{12}\,(2\gamma+\beta)\alpha\Big] \\ &\quad + {R_1}^3R_2(1-\cos\tau_{12})\,\sin(\sigma_2+\tau_2)\,(2\alpha+\gamma)\beta\Big\}\,\frac{1}{\Delta^{2\omega-2}}\,. \end{aligned} \tag{3.14}$$

where $\tau_{12}=\tau_1-\tau_2$ and

$$\begin{aligned} \Delta = {}& (1-\gamma)\gamma({R_1}^2+{R_1}^2+h^2) + 2\alpha\beta\,{R_2}^2(1-\cos\tau_{12}) \\ & -2R_1R_2\Big(\alpha\gamma\cos(\sigma_2+\tau_1)+\beta\gamma\cos(\sigma_2+\tau_2)\Big) \end{aligned} \tag{3.15}$$

In order to split off the divergent part of the integral we make use of the following key identity for the integrand of (3.14)

$$\begin{aligned} &E(\tau_1,\tau_2)\Big\{-R_1R_2\,(1+\cos(\sigma_2+\tau_1))\,\Big[R_1R_2\sin(\sigma_2+\tau_2)\,(2\alpha+\beta)\gamma \\ &+{R_1}^2\sin\tau_{12}\,(2\gamma+\beta)\alpha\Big] + {R_1}^3R_2(1-\cos\tau_{12})\,\sin(\sigma_2+\tau_2)\,(2\alpha+\gamma)\beta\Big\}\,\frac{1}{\Delta^{2\omega-2}} = \\ &-\tfrac{1}{2}\,{R_1}^2\,\partial_{\tau_2}\left(E(\tau_1,\tau_2)\,\frac{1-\cos\tau_{12}}{\Delta^{2\omega-3}}\right) + R_1R_2\,\partial_{\tau_1}\left(E(\tau_1,\tau_2)\,\frac{1+\cos(\sigma_2+\tau_1)}{\Delta^{2\omega-3}}\right) \\ &+\tfrac{1}{2}\,R_1R_2\,\partial_{\tau_2}\left(E(\tau_1,\tau_2)\,\frac{1+\cos(\sigma_2+\tau_1)}{\Delta^{2\omega-3}}\right) + (\mathrm{IY})_{\mathrm{SE}} + (\mathrm{IY})_1 + (\mathrm{IY})_2 + (\mathrm{IY})_{\omega-2} \end{aligned} \tag{3.16}$$

where

$$\begin{aligned} (\mathrm{IY})_{\mathrm{SE}} &= \frac{2\pi\delta(\tau_{12})}{2\omega-3}\,R_1R_2\,\frac{1+\cos(\sigma_2+\tau_1)}{\Delta^{2\omega-3}} \\ (\mathrm{IY})_1 &= -\frac{1}{2\omega-3}\left\{{R_1}^2\,\frac{1-\cos\tau_{12}}{\Delta^{2\omega-3}} + R_1R_2\,\frac{1+\cos(\sigma_2+\tau_1)}{\Delta^{2\omega-3}}\right\} \\ (\mathrm{IY})_2 &= \frac{E(\tau_1,\tau_2)}{\Delta^{2\omega-2}}\,\Big[(R_1+R_2)^2+h^2\Big]\,\gamma\,(1-\gamma)\,\Big[R_1R_2\,\sin(\sigma_2+\tau_1) - \tfrac{1}{2}\,{R_1}^2\,\sin\tau_{12}\Big] \\ (\mathrm{IY})_{\omega-2} &= \frac{2\omega-4}{2\omega-3}\,\frac{E(\tau_1,\tau_2)}{\Delta^{2\omega-3}}\,\Big\{\tfrac{1}{2}\,{R_1}^2\,\sin\tau_{12} - R_1R_2\,\sin(\sigma_2+\tau_1)\Big\} \end{aligned} \tag{3.17}$$

which holds under integration over the angles τ_1,τ_2,σ_2 and the Feynman parameters α,β,γ. Plugging this relation back into (3.14) one sees that the total derivative terms of the right-hand-side of the identity (3.16) drop out. Moreover one can show that the integral over $(\mathrm{IY})_{\omega-2}$ is finite in $2\omega=4$ dimensions, therefore due to the $(2\omega-4)$ prefactor this term drops out as well.

To continue let us investigate the contribution of the $(\mathrm{IY})_{\mathrm{SE}}$ term coupling to the δ-function. Here the Feynman parameter integral factorizes and may be performed to yield

$$\begin{aligned}\int (\mathrm{IY})_{\mathrm{SE}} &= 2\pi\,(\mathrm{I})\int_0^{2\pi} d\sigma_2 d\tau_1 \frac{\Gamma(2\omega-2)\,R_1R_2}{2^5\pi^{2\omega}(2\omega-3)}\,\frac{1+\cos(\sigma_2+\tau_1)}{[{R_1}^2+{R_2}^2+h^2-2R_1R_2\,\cos(\sigma_2+\tau_2)]^{2\omega-3}}\\ &\quad\times\int_0^1 d\alpha d\beta d\gamma\,\frac{(\alpha\beta\gamma)^{\omega-2}\,\delta(\alpha+\beta+\gamma-1)}{(\gamma(1-\gamma))^{2\omega-3}}\\ &= -2\pi\,(\mathrm{I})\,\frac{\Gamma^2(\omega-1)}{2^5\pi^{2\omega}\,(2-\omega)\,(2\omega-3)}\int d\sigma_2 d\tau_1\,\frac{\dot{x}_1\cdot\dot{y}_2-R_1R_2}{[(x_1-y_2)^2]^{2\omega-3}} = -\frac{1}{2}\end{aligned}$$  (3.18)

where we have undone the parameterization of (2.5) in the second step. In the last step we see that upon using (3.13) this part of the IY-graph precisely cancels half of the self-energy graph (3.8). The second half comes from the mirror IY^T-graph which may be obtained from the above by swapping $R_1 \leftrightarrow R_2$. To summarize we thus have

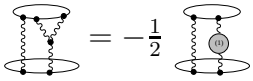 $= -\frac{1}{2}$ $+ \int(\mathrm{IY})_1 + \int(\mathrm{IY})_2$ (3.19)

in a symbolic notation.

For the evaluation of the $(\mathrm{IY})_1$ contribution we go back to exactly $2\omega = 4$ dimensions: $(\mathrm{IY})_1$ turns out to be finite. We found it useful to reintroduce the integral over r in (3.11) again and remove the Feynman parameters. One may then treat the angular integrals by contour techniques and is left with an integral over the space-point r. Doing this one starts with

$$\int(\mathrm{IY})_1 = -\frac{(\mathrm{I})}{2^5\pi^6}\int_0^{2\pi} d\tau_1 d\tau_2 d\sigma_2 \int d^4r\,\frac{\dot{x}_1\cdot\dot{x}_2-{R_1}^2+\dot{x}_1\cdot\dot{y}_2-R_1R_2}{(x_1-r)^2\,(x_2-r)^2\,(y_2-r)^2}\,. \tag{3.20}$$

Noting that in four dimensions the symbol (I) takes the value

$$(\mathrm{I})_{\omega=2} = \frac{g^6N(N^2-1)}{32\pi}\,\left[1-\sqrt{\tfrac{(R_1+R_2)^2+h^2}{(R_1-R_2)^2+h^2}}\,\right] \tag{3.21}$$

and performing the angular integrals leads to the final result

$$\begin{aligned}\int(\mathrm{IY})_1 = -\frac{g^6N(N^2-1)}{256\pi^3}\,&\left[1-\sqrt{\tfrac{(R_1+R_2)^2+h^2}{(R_1-R_2)^2+h^2}}\,\right]\int_0^\infty d\rho\int_{-\infty}^\infty dr_3\int_{-\infty}^\infty dr_4\frac{1}{\rho\,L_1\,\sqrt{L_2^h}}\\ &\times\Big[\rho^4+h^2\,(\sqrt{L_1}-\rho^2-R_1^2-r_3^2-r_4^2)+2\,h\,r_3\,(-\sqrt{L_1}+\rho^2+R_1^2+r_3^2+r_4^2)\\ &-(\sqrt{L_1}-R_1^2-r_3^2-r_4^2)\,(\sqrt{L_2^h}+2\,R_1^2-R_2^2+r_3^2+r_4^2)\\ &-\rho^2\,(\sqrt{L_1}-\sqrt{L_2^h}+5\,R_1^2+4\,R_1\,R_2+R_2^2-2\,(r_3^2+r_4^2))\Big]\end{aligned} \tag{3.22}$$

where we have introduced

$$\begin{aligned}L_1 &= \Big[(\rho-R_1)^2+r_3^2+r_4^2\Big]\,\Big[(\rho+R_1)^2+r_3^2+r_4^2\Big]\\ L_2^h &= \Big[(\rho-R_2)^2+(r_3-h)^2+r_4^2\Big]\,\Big[(\rho+R_2)^2+(r_3-h)^2+r_4^2\Big]\,.\end{aligned} \tag{3.23}$$

Note that due to the symmetry of our loop configuration in the $1-2$ plane one is able to reduce (3.20) to a three dimensional integral. This is as far as one can get analytically – (3.22) may be evaluated with good precision numerically. We will return to an analytical treatment of (3.22) in the potential limit.

Turning to the $(\mathrm{IY})_2$ contribution one finds the following compact expression via a derivative with respect to h^2

$$\int(\mathrm{IY})_2 = \frac{(\mathrm{I})}{2^5\pi^6}\,\frac{\partial}{\partial h^2}\,\left[\int_0^{2\pi} d\tau_1 d\tau_2 d\sigma_2\, E(\tau_1,\tau_2)\,\int d^4r\,\frac{\dot{y}_2\cdot x_1+\frac{1}{2}\,\dot{x}_2\cdot x_1}{(x_1-r)^2\,(x_2-r)^2\,(y_2-r)^2}\right] \tag{3.24}$$

after reintroducing the r integration. Now the integration over the angles is less straightforward due to the path ordering symbol $E(\tau_1,\tau_2)$. The calculation proceeds along lines similar to the three-ladder case: One introduces complex variables $(z,w_1,w_2)=(e^{i\sigma_2},e^{i\tau_1},e^{i\tau_2})$ and rewrites the loop part of eq.(3.24) as a multiple, open contour integral:

$$\begin{aligned}
\int(\mathrm{IY})_2 &= \frac{(\mathrm{I})}{2^6\pi^6}\,\frac{1}{R_1R_2}\int d^4r\,\frac{1}{r_1-ir_2}\,\frac{1}{r_1^2+r_2^2}\,\frac{\partial}{\partial h^2}\,\oint\frac{dz}{iz}\oint\frac{dw_2}{iw_2}\,\{\quad\}\\
&\text{where}\\
\{\quad\} &= \left[-4\pi i\int_1^{w_2}\frac{dw_1}{iw_1}+\oint\frac{dw_1}{iw_1}\,(\log w_1-\log w_2)\right]\times\\
&\quad\times\frac{R_1\,z\,(w_2^2-w_1^2)+2\,R_2\,w_2\,(w_1^2z^2-1)}{(z-z_-)(z-z_+)(w_1-w_-)(w_1-w_+)(w_2-w_-)(w_2-w_+)}
\end{aligned} \tag{3.25}$$

Here $z_\pm$,$w_\pm$ are, respectively, the roots of the quadratic equations

$$\begin{aligned}
z^2-\frac{1}{R_2}\,\frac{R_2^2+\rho^2+(r_3-h)^2+r_4^2}{r_1+ir_2}\,z+\frac{r_1-ir_2}{r_1+ir_2}&=0\\
w^2-\frac{1}{R_1}\,\frac{R_1^2+\rho^2+r_3^2+r_4^2}{r_1-ir_2}\,w+\frac{r_1+ir_2}{r_1-ir_2}&=0
\end{aligned} \tag{3.26}$$

Now the integrations on w_2,w_1 are elementary, if tedious, and the z-integration can be performed by the residue theorem. The final expression is

$$\begin{aligned}
\int(\mathrm{IY})_2 = \frac{g^6N(N^2-1)}{64\pi^3}\,&\left[1-\sqrt{\tfrac{(R_1+R_2)^2+h^2}{(R_1-R_2)^2+h^2}}\right]\,\left[h^2+(R_1+R_2)^2)\right]\\
&\times\int_0^\infty d\rho\int_{-\infty}^\infty dr_3\int_{-\infty}^\infty dr_4\,\frac{h-r_3}{h\,\rho\,\sqrt{L_1}(L_2^h)^{3/2}}\,\Big\{\rho^4+h^2\,(R_1^2+\rho^2+r_3^2+r_4^2)\\
&-2\,h\,r_3\,(R_1^2+\rho^2+r_3^2+r_4^2)+(R_1^2+r_3^2+r_4^2)\,(R_2^2+r_3^2+r_4^2)\\
&+\rho^2\left(R_1^2-3\,R_2^2+2\,(r_3^2+r_4^2)\right)\Big\}\\
&\times\log\left[2+\frac{\sqrt{L_1}\,(R_1^2+\rho^2+r_3^2+r_4^2)-(R_1^2+\rho^2+r_3^2+r_4^2)^2}{2\rho^2\,R_1^2}\right]
\end{aligned} \tag{3.27}$$

which completes the computation of the IY-graphs.

As already mentioned above, this integral still has a residual logarithmic divergence unless $R_1 = R_2$. However, one can show that for $R_1 \neq R_2$ this divergence is precisely canceled by the analogous divergence coming from $(\mathrm{IY}^T)_2$.

3.4 The X-Graph

The next graph on our list is the X-graph. Let us denote the two points on the upper loop by $x_i(\tau_i)$ and the two points on the lower loop by $y_i(\sigma_i)$ $(i = 1, 2)$. Happily no path ordering is required and the graph turns out to be finite in four dimensions. After taking care of combinatorial factors and performing the usual Wick contractions one arrives at

$$
\begin{aligned}
&= \tfrac{g^6 N(N^2-1)}{8} \int_0^{2\pi} d\tau_1\, d\tau_2\, d\sigma_1\, d\sigma_2 \\
&\quad \times \Big[(\dot{x}_1 \cdot \dot{y}_2 - R_1\, R_2)\, (\dot{y}_1 \cdot \dot{x}_2 - R_1\, R_2) - (\dot{x}_1 \cdot \dot{x}_2 - {R_1}^2)\, (\dot{y}_1 \cdot \dot{y}_2 - {R_2}^2) \Big] \\
&\quad \times \tfrac{1}{(4\pi^2)^4} \int d^4 r \frac{1}{(x_1 - r)^2\, (x_2 - r)^2\, (y_1 - r)^2\, (y_2 - r)^2}
\end{aligned}
\tag{3.28}
$$

Leaving the r integral untouched for the moment, we first perform the four angular integrals over τ_i and σ_i which are all elementary. One then obtains the following compact result

$$
\begin{aligned}
&= \frac{g^6 N(N^2-1)}{256\pi^3} \int_0^\infty d\rho \int_{-\infty}^\infty dr_3 \int_{-\infty}^\infty dr_4\, \frac{1}{\rho\, L_1\, L_2^h} \Big[-h^2\, R_1 + \sqrt{L_2^h}\, R_1 \\
&\qquad + \sqrt{L_1}\, R_2 + 2\, h\, R_1\, r_3 - (R_1 + R_2)\, (\rho^2 + R_1\, R_2 + r_3^2 + r_4^2) \Big]^2
\end{aligned}
\tag{3.29}
$$

where we again made use of the abbreviations (3.23) for L_1 and L_2^h. The integrations over ρ, r_3 and r_4 appear to be not expressable in terms of known functions.

3.5 The H-Graph

For the computation of the H-graph we denote the two points on the upper loop by $x_i(\tau_i)$ and the two points on the lower loop by $y_i(\sigma_i)$ $(i = 1, 2)$. Again there is no path ordering for this graph, and it is completely finite due to cancellations between gauge and scalar degrees of freedom, allowing us to work in four dimensions from the outset. One then starts off with the following integral

$$
\begin{aligned}
&= \tfrac{g^6 N(N^2-1)}{8} \int_0^{2\pi} d\tau_1\, d\tau_2\, d\sigma_1\, d\sigma_2 \\
&\quad \times \Big[2\, \dot{y}_1^M\, \dot{x}_1 \cdot \partial_{y_1} - 2\, \dot{x}_1^M\, \dot{y}_1 \cdot \partial_{x_1} + (\dot{x}_1 \cdot \dot{y}_1 - R_1 R_2)\, (\partial_{x_1^M} - \partial_{y_1^M}) \Big] \\
&\quad \times \Big[2\, \dot{y}_2^M\, \dot{x}_2 \cdot \partial_{y_2} - 2\, \dot{x}_2^M\, \dot{y}_2 \cdot \partial_{x_2} + (\dot{x}_2 \cdot \dot{y}_2 - R_1 R_2)\, (\partial_{x_2^M} - \partial_{y_2^M}) \Big] \\
&\quad \times \tfrac{1}{(4\pi^2)^5} \int d^4 z\, d^4 w\, \frac{1}{(x_1 - z)^2\, (y_1 - z)^2\, (z - w)^2\, (x_2 - w)^2\, (y_2 - w)^2}
\end{aligned}
\tag{3.30}
$$

where we have made use of a handy five dimensional index ($M = \mu, 5$) notation where $\dot{x}_i^M = (\dot{x}_i^\mu, |\dot{x}_i|)$ and $\partial_{x_i^M} = (\partial_{x_i^\mu}, 0)$. As usual we will now perform the angular integrals $(\tau_1, \tau_2, \sigma_1, \sigma_2)$ and leave the space-integrals over z and w untouched. The angular integration factorizes and one is left with the computation of the five dimensional vector $H^M(z)$

$$H^M(z) \equiv \int_0^{2\pi} d\tau\, d\sigma\, \Big[2\,\dot{y}^M\,\dot{x}\cdot\partial_y - 2\,\dot{x}^M\,\dot{y}\cdot\partial_x + (\dot{x}\cdot\dot{y} - R_1R_2)\,(\partial_{x^M} - \partial_{y^M})\Big] \times \frac{1}{(x-z)^2\,(y-z)^2}\,. \tag{3.31}$$

After taking the derivatives in (3.31) and inserting the parameterization (2.5) all angular integrals are elementary and may be performed straightforwardly. Interestingly enough one finds the following identity

$$\int_0^{2\pi} d\tau\, d\sigma\, \frac{\dot{y}^M\,\dot{x}\cdot(\dot{y}-z)}{(x-z)^2\,[(y-z)^2]^2} = \int_0^{2\pi} d\tau\, d\sigma\, \frac{\dot{x}^M\,\dot{y}\cdot(\dot{x}-z)}{[(x-z)^2]^2\,(y-z)^2} \tag{3.32}$$

which lets the fifth component of H^M vanish and reduces (3.31) to

$$H^\mu(z) = -2\int_0^{2\pi} d\tau\, d\sigma\, \frac{\dot{x}\cdot\dot{y} - R_1R_2}{(x-z)^2\,(y-z)^2}\,\left[\,\frac{x^\mu - z^\mu}{(x-z)^2} - \frac{y^\mu - z^\mu}{(y-z)^2}\,\right]. \tag{3.33}$$

Using this the full H-graph may be represented as

$$= \tfrac{g^6N(N^2-1)}{8}\;\tfrac{1}{(4\pi^2)^5}\;\int d^4z\,d^4w\,\frac{H(z)\cdot H(w)}{(z-w)^2} \tag{3.34}$$

Performing the angular integrations in (3.33) one finds $H^\mu(r) = (r_1\,H^\rho, r_2\,H^\rho, H^3, H^4)$ where

$$\begin{aligned}
H^\rho = -\frac{2}{\rho}\Big[&\frac{4\,\pi^2\,\rho\,R_1\,R_2\,(-R_1+\sqrt{\rho^2+r_3^2+r_4^2})\,(R_1+\sqrt{\rho^2+r_3^2+r_4^2})}{L_1^{3/2}\,\sqrt{L_2^h}}\\
&-\frac{4\,\pi^2\,r\,R_1\,R_2\,(h^2+\rho^2-R_2^2-2\,h\,r_3+r_3^2+r_4^2)}{\sqrt{L_1}\,(L_2^h)^{3/2}}\\
&+\frac{\pi^2\,(-\sqrt{L_2^h}+\rho^2+R_2^2+(h-r_3)^2+r_4^2}{2\,L_1^{3/2}\,\sqrt{L_2^h}\,\rho^3}\,\Big(-L_1^{3/2}+8\,\rho^4\,R_1^2-8\,\rho^2\,R_1^4+R_1^6\\
&-8\,\rho^2\,R_1^2\,(\rho^2+r_3^2+r_4^2)+3\,R_1^4\,(\rho^2+r_3^2+r_4^2)+3\,R_1^2\,(\rho^2+r_3^2+r_4^2)^2+(\rho^2+r_3^2+r_4^2)^3\Big)\\
&+\frac{\pi^2\,(-1+(\rho^2+R_1^2+r_3^2+r_4^2)/\sqrt{L_1})}{2\,(L_2^h)^{3/2}\,\rho^3}\,\Big(-h^6+(L_2^h)^{3/2}-\rho^6+6\,h^5\,r_3\\
&-3\,\rho^4\,(R_2^2+r_3^2+r_4^2)-(R_2^2+r_3^2+r_4^2)^3-3\,h^4\,(\rho^2+R_2^2+5\,r_3^2+r_4^2)\\
&+4\,h^3\,r_3\,(3\,\rho^2+3\,R_2^2+5\,r_3^2+3\,r_4^2)+\rho^2\,(R_2^2+r_3^2+r_4^2)\,(5\,R_2^2-3\,(r_3^2+r_4^2))\\
&-h^2\,(3\,\rho^4-2\,\rho^2\,(R_2^2-9\,r_3^2-3\,r_4^2)+3\,(R_2^2+r_3^2+r_4^2)\,(R_2^2+5\,r_3^2+r_4^2))\\
&+2\,h\,r_3\,\Big\{3\,\rho^4+3\,(R_2^2+r_3^2+r_4^2)^2+\rho^2\,(-2\,R_2^2+6\,(r_3^2+r_4^2))\Big\}\Big)\Big]
\end{aligned} \tag{3.35}$$

and

$$H^3 = -\frac{8\,\pi^2}{L_1^{3/2}\,(L_2^h)^{3/2}}\Big[L_1\,R_1\,R_2\,(h-r_3)\,(R_2^2+(h-r_3)^2+r_4^2+\rho^2)$$
$$+L_2^h\,R_1^2\,r_3\,(-\sqrt{L_2^h}+R_2^2+(h-r_3)^2+r_4^2+\rho^2)+L_2^h\,R_1\,R_2\,r_3\,(R_1^2+r_3^2+r_4^2+\rho^2)$$
$$+L_1\,R_2^2\,(h-r_3)\,(-\sqrt{L_1}+R_1^2+r_3^2+r_4^2+\rho^2)\Big] \tag{3.36}$$

and

$$H^4 = -\frac{8\,\pi^2\,r_4}{L_1^{3/2}\,(L_2^h)^{3/2}}\Big[-(L_2^h)^{3/2}\,R_1^2+h^2\,R_1\,(L_2^h\,R_1-L_1\,R_2)-2\,h\,R_1\,(L_2^h\,R_1-L_1\,R_2)\,r_3$$
$$+L_2^h\,R_1\,(R_1+R_2)\,(R_1\,R_2+r_3^2+r_4^2+\rho^2)+L_1\,R_2\,(\sqrt{L_1}\,R_2$$
$$-(R_1+R_2)\,(R_1\,R_2+r_3^2+r_4^2+\rho^2))\Big] \tag{3.37}$$

with $\rho^2 = r_1^2+r_2^2$. Again this is as far as one gets analytically for the general geometry – a number of further integrals may be performed in (3.34) in the flat ($h = 0$) or "cake" ($R_1 = R_2$) cases.

3.6 Putting Everything Together

We have thus shown for our geometry that, due to subtle cancellations, the Maldacena-Wilson loop is completely finite to $\mathcal{O}(g^6)$. Let us now verify whether or not the finite parts of non-ladder diagrams cancel as well: We simply have to add the finite contributions of the interactive graphs worked out in sections 3.2 -3.5. For simplicity, as discussed above, we will content ourselves with the case $R := R_1 = R_2$, $h \neq 0$. The quickest, yet safe way to arrive at the answer is to numerically compute the contributions of all finite parts for some specific values of R and h and to subsequently add the obtained numbers. This can be done with great accuracy since our final expressions are finite, low dimensional integrals. We tested various combinations of R and h and found that the sum of finite parts yields in all instances a non-zero number, exceeding the margin of error by many orders of magnitude. In conclusion, to $\mathcal{O}(g^6)$ non-ladder diagrams no longer cancel. Therefore no unknown "non-renormalization theorem" is at work, and we explicitly demonstrated that the quite amazing $\mathcal{O}(g^4)$ cancellations observed in the calculations of [7] are *not* generic. Our ultimate goal, however, is to verify whether internal vertex diagrams contribute to the static potential in order to explain the discrepancy between eqs.(1.3) and (1.4). We will now apply our results to obtain some new insights into this question.

4. The Static Potential Limit

The geometric set-up analyzed in this work is clearly sufficiently rich to recover the case of infinite, anti-parallel lines, corresponding to the static potential limit: We

simply take the radii of the circles to infinity while keeping their separation finite. Luckily, in this limit the contributions of all graphs found above can be worked out explicitly. We can therefore analytically demonstrate the non-cancellation of internal vertex diagrams, serving as a check on the numerical result of the previous section. We will take the following limiting procedure:

$$R_1 = R_2 =: R, \qquad T := 2\pi R \to \infty \qquad \text{while} \qquad L := h \to 0 \tag{4.1}$$

Let us briefly discuss the subtle issue of the precise definition of the static potential. For a rectangle, cf. section 1, the measured operator is a single loop and the usual definition is $V(L) = -1/T \log\langle \mathcal{W}[C]\rangle$. Clearly this assumes the loop operator to be of the form $\mathcal{W}[C] = \exp[V(L)\ T]$. Explicit calculations [6],[7] demonstrate that *perturbatively* this is not the case[2]. In our case, we should analogously define the static potential through $V(L) = -1/T \log\langle \mathcal{W}(C_1)\,\mathcal{W}(C_2)\rangle_c$. The just mentioned problem of the perturbative definition of $V(L)$ is further aggravated since now the connected two-loop correlator does not even exponentiate in terms of a power series in the gauge coupling g^2. We will therefore avoid any attempt to define $V(L)$ at weak coupling, and use the notion "static potential limit" simply as a *façon de parler* to denote the perturbative evaluation of $\langle \mathcal{W}[C]\rangle$ and $\langle \mathcal{W}(C_1)\,\mathcal{W}(C_2)\rangle_c$ in the geometric limit of infinite anti-parallel lines:

$$\langle \mathcal{W}(C_1)\,\mathcal{W}(C_2)\rangle_c\Big|_{\frac{T}{L}\to\infty} = \sum_{k=1}^{\infty} W_{2k}(T/L)\ g^{2k} \tag{4.2}$$

However, we do expect that at strong coupling $V(L)$ turns out to be well defined – at any rate, this is a prediction of AdS/CFT, cf. eq.(1.3).

Let us now find the first three coefficients $W_{2k}(T/L)$ in eq.(4.2) from the results of section 3. Applying the limiting procedure (4.1), W_2 and W_4 are immediately found from eqs.(2.9),(2.10):

$$W_2 = \frac{g^2 N}{4\pi}\ \frac{T}{L} \tag{4.3}$$

and

$$W_4 = \frac{g^4 N^2}{32\ \pi^2}\Big(\frac{T}{L}\Big)^2 - \frac{g^4 N^2}{32\ \pi}\frac{T}{L} \tag{4.4}$$

To two-loop order the contributions of the ladder graphs are directly obtained from the explicit results eqs.(3.1),(3.4),(3.5):

$$W_6^{\text{ladders}} = \frac{g^6 N^3}{384\ \pi^3}\Big(\frac{T}{L}\Big)^3 - \frac{g^6 N(N^2-1)}{32\ \pi^4}\ \Big(\frac{T}{L}\Big)^2\Big(\ \log\Big(4\pi\frac{T}{L}\Big) + 1\ \Big)$$
$$+\frac{g^6 N(N^2-1)}{32\ \pi^3}\ \frac{T}{L}\ \log\ \frac{T}{L} + \mathcal{O}\Big(\frac{T}{L}\Big) \tag{4.5}$$

[2]E.g. at $\mathcal{O}(g^4)$ a term $\frac{T}{L}\log\frac{T}{L}$ appears. There is some discussion in [6],[7] arguing that this term should be replaced by $\frac{T}{L}\log\frac{1}{\lambda}$. It is not obvious to us whether this is fully consistent, and in particular how to extend this procedure to higher loops.

where we did not write out the subleading terms growing like T/L and $\log T/L$.

Let us now investigate the contributions of the non-ladder diagrams in the static potential limit. In the limit (4.1) the finite parts of the IY-graph integrals (3.22) and (3.27) are dominated by the region around $\rho \sim R$, $r_3 \sim 0, h$ and $r_4 \sim 0$. The leading contribution in the static potential limit may then be extracted from the reduced integrals

$$\begin{aligned} \int (\mathrm{IY})_1 \Big|_{\frac{T}{L}\to\infty} &= -\frac{g^6 N(N^2-1)}{128\pi^3}\,\frac{R}{h} \int_0^\infty d\rho \int_{-\infty}^{\infty} dr_3 \int_{-\infty}^{\infty} dr_4 \\ &\qquad \times \frac{1}{(\rho-R)^2 + r_3^2 + r_4^2}\,\frac{1}{[\,(\rho-R)^2 + (r_3-h)^2 + r_4^2\,]^{1/2}} \\ &= -\frac{g^6 N(N^2-1)}{64\pi^3}\,\frac{T}{L}\log\frac{T}{L} + \mathcal{O}\left(\frac{T}{L}\right) \end{aligned} \tag{4.6}$$

and

$$\begin{aligned} \int (\mathrm{IY})_2 \Big|_{\frac{T}{L}\to\infty} &= -\frac{g^6 N(N^2-1)}{64\pi^3} \int_0^\infty d\rho \int_{-\infty}^{\infty} dr_3 \int_{-\infty}^{\infty} dr_4 \\ &\qquad \times \frac{h - r_3}{[\,(\rho-R)^2 + r_3^2 + r_4^2\,]^{1/2}}\,\frac{\log[\,2\,\frac{[\,(\rho-R)^2+r_3^2+r_4^2\,]^{1/2}}{R}\,]}{[\,(\rho-R)^2 + (r_3-h)^2 + r_4^2\,]^{3/2}} \\ &= \frac{g^6 N(N^2-1)}{32\pi^2}\,\log\frac{T}{L} + \mathcal{O}(1)\,. \end{aligned} \tag{4.7}$$

telling us that this graph is dominated by the $(\mathrm{IY})_1$ piece in the $T/L \to \infty$ limit. The mirror IY^T-graph yields the same contributions (4.6) and (4.7) to the static potential limit. Turning to the X-graph in the limit (4.1) one finds from (3.29) the leading behaviour

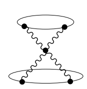

$$\begin{aligned} \Big|_{\frac{T}{L}\to\infty} &= \frac{g^6 N(N^2-1)\,R}{256\pi^3} \int_0^\infty d\rho \int_{-\infty}^{\infty} dr_3 \int_{-\infty}^{\infty} dr_4 \\ &\qquad \times \frac{1}{(\rho-R)^2 + r_3^2 + r_4^2}\,\frac{1}{(\rho-R)^2 + (r_3-h)^2 + r_4^2} \\ &= \frac{g^6 N(N^2-1)}{512\pi}\,\frac{T}{L} + \mathcal{O}\left(\log\frac{T}{L}\right)\,. \end{aligned} \tag{4.8}$$

In order to extract the static potential limit of the H-graph it is technically preferable to consider a different limit than (4.1) and rather take

$$h = 0, \qquad T := 2\pi R_2 \to \infty \qquad \text{while} \qquad L := |R_2 - R_1| \to 0\,, \tag{4.9}$$

which leads to rotational symmetry also in the 3-4 plane. For the leading contribution in T/L this limit is completely equivalent to (4.1). Introducing σ as the radius in

the 3-4 plane, the integral (3.34) reduces in this flat geometry to

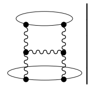

$$\Big|_{h=0} = \frac{g^6 N(N^2-1)}{8\cdot(4\pi^2)^4} \int_0^\infty d\rho\, d\bar\rho\, d\sigma\, d\bar\sigma \int_0^{2\pi} d\phi\, d\theta\, \rho\, \bar\rho\, \sigma\, \bar\sigma \times \frac{H^\rho\, H^{\bar\rho}\, \rho\, \bar\rho\, \cos\phi + H^\sigma\, H^{\bar\sigma}\, \sigma\bar\sigma\, \cos\theta}{\rho^2+\bar\rho^2+\sigma^2+\bar\sigma^2 - 2\rho\,\bar\rho\, \cos\phi - 2\sigma\,\bar\sigma\, \cos\theta} \qquad (4.10)$$

where the barred and unbarred quantities are associated with the 1-2 and 3-4 plane radii of the space-points w and z of (3.34) respectively, and ϕ and θ are the relative angles. In the limit (4.9) this integral is dominated by the region $(\rho,\bar\rho) \sim [R_1,R_2]$, $(\sigma,\bar\sigma) \sim 0$, $\phi \sim 0$ and $\theta \in [0,2\pi]$. Within this region the functions H^ρ and H^σ following from (3.35),(3.36),(3.37) read

$$\begin{aligned} H^\rho &= 2\pi^2\, \frac{R_1-R_2}{R_1+R_2}\, \frac{(\rho-R_1)\,(\rho-R_2)}{[\,(\rho-R_1)^2+\sigma^2\,]^{3/2}\,[\,(\rho-R_2)^2+\sigma^2\,]^{3/2}} \\ H^\sigma &= 2\pi^2\,(R_1-R_2)\, \frac{\rho-(R_1+R_2)/2}{[\,(\rho-R_1)^2+\sigma^2\,]^{3/2}\,[\,(\rho-R_2)^2+\sigma^2\,]^{3/2}} \end{aligned} \qquad (4.11)$$

Plugging (4.11) into the static potential limit of (4.10) and performing the integral over θ one discovers that the dependence on T/L may be scaled out of the integral. Finally one has

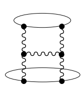

$$\Big|_{\frac{T}{L}\to\infty} = c\cdot g^6 N(N^2-1)\,\frac{T}{L} + \mathcal{O}\left(\log\frac{T}{L}\right) \qquad c = 7.23(9)\cdot 10^{-5} \qquad (4.12)$$

where c is a number expressed through a finite yet complicated five dimensional integral independent of T/L, which we evaluated numerically.

To summarize, we have thus analytically proven the non-cancellation of the internal vertex diagrams. In particular, we notice that the T/L behavior is different for the various graphs: Independently of the symmetry factor they cannot possibly cancel. The strongest contribution in the non-ladder sector comes from the IY-graph so that

$$W_6^{\text{non-ladders}} = -\frac{g^6 N(N^2-1)}{32\,\pi^3}\,\frac{T}{L}\,\log\frac{T}{L} + \mathcal{O}\left(\frac{T}{L}\right) \qquad (4.13)$$

which presicely cancels the subleading $T/L\,\log T/L$ ladder-term in (4.5).

Despite the fact that the non-ladder-diagrams do not cancel, our results indicate that their contribution to the limit of infinite anti-parallel lines is rather weak (at $\mathcal{O}(g^6)$ $T/L\,\log T/L$ vs. $(T/L)^3$). Unfortunately their quantitative influence on the strong coupling potential is difficult to estimate. Naively, one could speculate that the fact that the vertex contributions are strongly subleading might explain the near coincidence of eqs.(1.3),(1.4). However the issue is rather subtle: In the planar $(N=\infty)$ limit we expect that summing up perturbation theory correctly reproduces

the non-perturbative physics[3]. In principle it is therefore conceivable that the ladder-approximation still captures the correct gauge-theory result in the large N, strong-coupling and $T/L \to \infty$ limits. If true, and if eq.(1.4) is correct this would contradict the AdS/CFT prediction eq.(1.3). Clearly we need to increase our understanding on how the subleading terms in the T/L expansion of the coefficients W_{2k} influence the strong coupling static potential extracted from eq.(4.2). This will be left for future work.

5. Outlook

The AdS/CFT correspondence has been inspiring since it appears to allow for analytic calculations in strongly coupled $U(N)$ gauge theory, at least when N is infinite and $\mathcal{N}$ (the number of supersymmetries) is large ($\mathcal{N} = 4$). However, we feel more attempts should be made to state the consequences of the correspondence for the gauge theory more precisely in order to perform quantitative, non-kinematical analytic tests. A perfect comparison would be to use supersymmetry to obtain a non-trivial strong coupling result on the gauge theory side that unequivocally agrees with the "corresponding" classical supergravity computation. Clearly non-unitary Maldacena-Wilson loops, as opposed to ordinary unitary Wilson loops, are perfect candidates for such a test: They appear to be completely *finite gauge invariant* observables with intriguing properties on both sides of the correspondence. As such, they deserve to be much more carefully studied:

• To date, no rigorous proof exists in $\mathcal{N} = 4$ gauge theory that all perturbative corrections cancel in the case of a straight line:

$$\langle \mathcal{W}[C] \rangle = 1, \qquad C = \text{straight line}. \tag{5.1}$$

• It has been argued in [8] but by no means proven that only ladder diagrams contribute to a circular Maldacena-Wilson loop for all finite gauge groups $U(N)$ and $SU(N)$ (see e.g. eq.(1.5)). If true this would lead to

$$\langle \mathcal{W}[C] \rangle = \frac{1}{N} L^1_{N-1}(-g^2/4)\ e^{g^2/8}, \qquad C = \text{circle}, \tag{5.2}$$

where L^1_{N-1} is a Laguerre polynomial of degree N in g^2. In [12] a variation of the anomaly arguments of [8] proposing a zero-dimensional matrix model description of the circular loop was considered. However, the relation of the considered matrix model potential to the full field theoretic problem remains unclear. An important

[3]There is a caveat: A large N phase transition, triggered by the increase in the number of non-planar diagrams, might take place at some finite value of the 't Hooft coupling $\lambda = Ng^2$: In that case the weak and strong coupling phase might turn out to be analytically unrelated, yielding one possible explanation for the discrepancy between the strong coupling ladder-approximation eq.(1.4) and the AdS/CFT result eq.(1.3).

further question is the strength of instanton contributions to the Maldacena-Wilson loop – preliminary results were reported in [13].

• The subtle cancellations of divergences found in this and previous work required a serious calculational effort; they are far from obvious. An all-orders result for arbitrary smooth contours would be very desirable. In fact one should prove the highly non-trivial property

$$0 < |\langle \mathcal{W}[C] \rangle| < \infty \qquad C = \text{(any?) contour.} \tag{5.3}$$

• A perfect quantitative test for the correspondence would be the verification of the strong coupling static potential as predicted by AdS/CFT: How to find in the gauge theory the non-trivial number in front of the Coulomb potential (see eq.(1.3))

$$V(L) \sim 4\,\pi^2\,\Gamma^{-4}(1/4)\;L^{-1}\;? \tag{5.4}$$

In the present work we discussed some of the subtleties surrounding this major challenge. Our result shows that non-ladder diagrams are non-vanishing but subleading, and one wonders whether the ladder approximation of [6] could be improved in order to systematically approximate the correct result.

• Our results can also be used to consider the limit $R_2 \to 0$ and $h \gg R_1$, which should be related to the scenario of [14].

• There has been some confusion in the literature as to whether the Maldacena-Wilson loop operator (2.1) is the final object to be compared to supergravity. The issue is whether or not supersymmetry requires also fermionic degrees on the boundary.

• The existing perturbative studies do not make any explicit use of supersymmetry. In fact, in this work supersymmetry only entered in the fermionic contribution to the gauge/scalar self energy, and, quite indirectly, in the "BPS" property of the Maldacena-Wilson loop [11]. Is there a more appropriate gauge (e.g. Mandelstam-Leibbrandt) or a better technique (e.g. supergraphs) that renders higher order calculations feasible?

Acknowledgments.

The authors would like to thank G. Arutyunov, A. Hartl, S. Kuzenko, H. Nicolai, Y. Schröder, G. Semenoff, S. Silva and S. Theisen for useful discussions.

References

[1] G. 't Hooft, "A Planar Diagram Theory For Strong Interactions," Nucl. Phys. B **72** (1974) 461.

[2] J. Maldacena, "The large N limit of superconformal field theories and supergravity," Adv. Theor. Math. Phys. **2** (1998) 231 [Int. J. Theor. Phys. **38** (1998) 1113] [hep-th/9711200].

[3] J. Maldacena, "Wilson loops in large N field theories," Phys. Rev. Lett. **80** (1998) 4859 [hep-th/9803002].

[4] D. Berenstein, R. Corrado, W. Fischler and J. Maldacena, "The operator product expansion for Wilson loops and surfaces in the large N limit," Phys. Rev. D **59** (1999) 105023 [hep-th/9809188].

[5] O. Aharony, S. S. Gubser, J. Maldacena, H. Ooguri and Y. Oz, "Large N field theories, string theory and gravity," Phys. Rept. **323** (2000) 183 [hep-th/9905111].

[6] J. K. Erickson, G. W. Semenoff, R. J. Szabo and K. Zarembo, "Static potential in N = 4 supersymmetric Yang-Mills theory," Phys. Rev. D **61** (2000) 105006 [hep-th/9911088].

[7] J. K. Erickson, G. W. Semenoff and K. Zarembo, "Wilson loops in N = 4 supersymmetric Yang-Mills theory," Nucl. Phys. B **582** (2000) 155 [hep-th/0003055].

[8] N. Drukker and D. J. Gross, "An exact prediction of N = 4 SUSYM theory for string theory," hep-th/0010274.

[9] K. Zarembo, "Wilson loop correlator in the AdS/CFT correspondence," Phys. Lett. B **459** (1999) 527 [hep-th/9904149];
P. Olesen and K. Zarembo, "Phase transition in Wilson loop correlator from AdS/CFT correspondence," hep-th/0009210.

[10] K. Zarembo, "String breaking from ladder diagrams in SYM theory," JHEP **0103** (2001) 042 [hep-th/0103058].

[11] N. Drukker, D. J. Gross and H. Ooguri, "Wilson loops and minimal surfaces," Phys. Rev. D **60** (1999) 125006 [hep-th/9904191].

[12] G. Akemann and P. H. Damgaard, "Wilson loops in N = 4 supersymmetric Yang-Mills theory from random matrix theory," Phys. Lett. B **513** (2001) 179 [hep-th/0101225].

[13] M. Bianchi, M. B. Green and S. Kovacs, "Instantons and BPS Wilson loops," hep-th/0107028.

[14] G. W. Semenoff and K. Zarembo, "More exact predictions of SUSYM for string theory," hep-th/0106015.